Localization and clustering in atomic nuclei

Localization and clustering in atomic nuclei

J.-P. Ebran[1], E. Khan[2], T. Nikšić[3], D. Vretenar[3]

[1]CEA,DAM,DIF, F-91297 Arpajon, France

[2]Institut de Physique Nucléaire, Université Paris-Sud, IN2P3-CNRS, F-91406 Orsay Cedex, France

[3]Department of Physics, Faculty of Science, University of Zagreb, 10000 Zagreb, Croatia

Abstract. Nucleon localization and formation of clusters in nucleonic matter and finite nuclei are explored in a framework based on nuclear energy density functionals. The liquid-cluster transition is investigated and different measures of localization are discussed. The formation and evolution of α-clusters in excited states of both $N = Z$ and neutron-rich nuclei are analyzed. Effects of the spin-orbit coupling are discussed in relation to the confining potential.

1. Introduction

Localization of strongly interacting matter (baryons) and correlations that lead to formation of cluster structures in nucleonic matter, stellar matter, and finite nuclei is a topic at the forefront of experimental and theoretical research in nuclear physics and in astrophysical modelling [1, 2, 3, 4, 5, 6, 7]. The most simple system, infinite nuclear matter, consists of protons and neutrons only, and does not take into account electromagnetic interactions. At equilibrium (saturation) density it is a quantum liquid, however in dilute symmetric and asymmetric nuclear matter correlations induce formation of nucleon clusters. Matter in compact stellar objects, e.g. neutron stars, is characterized by the interplay of strong and electromagnetic interactions between the constituent hadrons and leptons, that leads to the formation of various phases of inhomogeneous matter, including cluster structures and the nuclear "pasta" phase [8, 9, 10] with neutrons and protons arranged in a variety of complex geometrical structures, e.g. cylindrical and planar, resembling different types of pasta. Finite nuclei, especially relatively light systems, exhibit a coexistence of the nucleonic liquid phase and nucleon clusters, predominantly ^{4}He nuclei (α-particles).

Clustering phenomena present a unique characteristic of nuclear structure and dynamics from light even-even systems with equal number of protons and neutrons to heavy and superheavy elements, and from stable nuclei to exotic neutron-rich systems far from the valley of β-stability. Some of the earliest models of nuclear structure were, in fact, formulated in terms of aggregates of nucleon clusters [11, 12, 13, 14]. Later it was suggested that although nucleonic matter in nuclei at low energies behaves like a quantum liquid, cluster structures should be observed as excited states close to the corresponding threshold energy for cluster emission [15, 16]. Closeness to the continuum and geometric shape transitions (intrinsic deformations) in light nuclei favour the formation of clusters. Their origin, however, lies in the effective nuclear interaction [17]. Very recently it has been shown, using lattice effective field theory, that in light even-even nuclei with equal numbers of protons and neutrons, a first-order transition at zero temperature occurs from a Bose-condensed gas of α-particles to a nuclear liquid [18]. The transition is determined by the strength of the $\alpha - \alpha$ interaction, which depends on the strength and locality of the nucleon-nucleon interactions. In an earlier study based on nuclear energy density functionals [19], we demonstrated that conditions for nucleon localization and formation of clusters can be related to the depth of the effective potential that confines protons and neutrons in a nucleus. To gain a full understanding of the mechanism of cluster formation, a consistent theoretical framework will have to be developed in the future that encompasses both cluster and quantum liquid-drop aspects, taking into account the principal characteristics of nuclei as finite, self-bound and open quantum systems: a relatively small number of constituent particles that self-consistently generate the confining potential, geometric shape transitions, surface effects, and coupling to the continuum.

2. Localization and clustering in nucleonic matter

Neutrons and protons in finite nuclei and extended nucleonic matter exhibit several phases. Symmetric nuclear matter, in particular, is an idealised infinite and homogeneous medium of equal number of structureless protons and neutrons interacting by low-energy nuclear forces, and no Coulomb force. At equilibrium nuclear matter behaves like a quantum (Fermi) liquid characterised by a saturation density of $\rho_0 \approx 0.16$ nucleon/fm^3 and binding energy $E_B \approx 16$ MeV/nucleon. The quantum liquid nature of nuclei and nuclear matter was discussed by B. Mottelson[20], who used a previously introduced quantality parameter [21]:

$$\Lambda_{\rm Mot} \hat{=} \frac{\hbar^2}{m\bar{r}^2|V_0|} \ , \tag{1}$$

The quantality $\Lambda_{\rm Mot}$ is defined as the ratio of the zero-point kinetic energy of the confined particle to its potential energy. The kinetic energy $\hbar^2/m\bar{r}^2$ corresponds to the momentum $p = \hbar/\bar{r}$, and the reduced mass $m/2$. The equilibrium inter-particle distance is $\bar{r}$, and $|V_0|$ denotes the depth of the potential. The transition between a solid phase (small kinetic energy compared to the potential at equlibrium) and a liquid (relatively large kinetic energy in comparison to the depth of the potential) occurs for $\Lambda_{\rm Mot} \simeq 0.1$. For small $\Lambda_{\rm Mot}$ the inter-particle interaction dominates and the equilibrium state of the many-body system will be a configuration in which each particle is localized with respect to its neighbours, whereas for $\Lambda_{\rm Mot} > 0.1$ the ground state is a quantum liquid in which the individual particles are delocalized and the low-energy excitations (quasi-particles) have infinite mean free path [22]. In the case of nuclear matter $\bar{r}$ is of the order of 1 fm, the strength of the bare nucleon-nucleon interaction $|V_0| \sim 100$ MeV, $mc^2 \simeq 940$ MeV is the nucleon mass and, therefore, $\Lambda_{\rm Mot} \simeq 0.4$ is a characteristic value for the nuclear quantum liquid phase.

At subsaturation densities correlations in strongly interacting matter lead to clustering phenomena [23] and, eventually, to a gas phase with nucleons and light clusters. As a result of strong correlations bound states are formed at low density and, when nucleonic bound states can be considered as bosons, that is, when formed from an even number of nucleons, Bose-Einstein condensation may occur at low temperatures in nuclear matter. In the spin singlet ($S = 0$) channel the interaction is not attractive enough to form a bound state. A bound proton-neutron pair, the deuteron, materializes in the triplet ($S = 1$) channel. However, as shown in Ref. [24], in the low-density limit the transition to triplet pairing does not take place because four-nucleon correlations dominate. In chemical equilibrium, at low temperatures in the low-density limit nuclear matter is characterised by condensation of α-particles (bound states of two protons and two neutrons) that are much more strongly bound than deuterons. The formation of well defined clusters is predicted at densities well below the saturation point. With increasing density clusters dissolve because of a reduction of their binding caused by the Pauli blocking that leads to the Mott effect for vanishing binding [25, 26].

3. Liquid-cluster transition in finite nuclei

When temperature decreases and density increases, a system of particles interacting through a short-range force undergoes a transition to a quantum liquid state [27]. Quantum effects become important when the typical dispersion of the constituent particles, that is, the thermal de Broglie wavelength of a particle $\lambda = h/p \simeq \hbar/\sqrt{2mkT}$ becomes comparable to the average inter-particle spacing. In a transition to a quantum liquid state the constituent particles are delocalized and the system reaches a homogeneous density (mean-field phase). Both the bosonic/fermionic nature of a many-body system and the inter-particle interaction determine characteristic properties of a quantum liquid [27]. In a finite isolated system in which temperature cannot be assigned unambiguously, the de Broglie wavelength can be defined for the motion of particles as $\lambda_{\rm dB} = 2\pi\hbar/\sqrt{2m(E-V)}$. For $E \sim 0$ and $V = -V_0$, the de Broglie wavelength can be related to Mottelson's quantality parameter [23]:

$$\lambda_{\rm dB} = \pi\bar{r}\sqrt{2\Lambda_{\rm Mot}} \tag{2}$$

The quantality parameter is defined for infinite homogeneous systems and, therefore, in the nuclear case it does not include any mass or size dependence. To analyze localization of single-nucleon wave functions in finite nuclei one needs to consider a quantity that is sensitive to both the nucleon number and size of a nucleus. In Ref. [19] we introduced the dimensionless parameter $\alpha_{\rm loc}$:

$$\alpha_{\rm loc} \hat{=} \frac{\Delta r}{\bar{r}} \tag{3}$$

where $\bar{r}$ is the average inter-nucleon distance, and Δr the spatial dispersion of the wave function:

$$\Delta r = \sqrt{\langle r^2\rangle - \langle r\rangle^2} \tag{4}$$

For large values of $\alpha_{\rm loc}$ the orbits of individual nucleons will be delocalized and the nucleus in the Fermi liquid phase. When $\alpha_{\rm loc}$ is very small nucleons can be localized on the nodes of a crystal-like structure. For $\alpha_{\rm loc} \approx 1$ the spatial dispersion of the single-nucleon wave function is of the same size as the inter-nucleon distance and, therefore, localization facilitates a transition from the quantum liquid phase to a hybrid phase of cluster states. For finite systems like nuclei this transition, of course, cannot be sharp and cluster states coexists with mean-field type states. The transition from the quantum liquid to the cluster phase is controlled by the specific dynamics and length scale of the system under consideration [19, 18] and, in particular, finite size effects are important.

When the confining nuclear potential is approximated by a 3-dimensional isotropic harmonic oscillator, the localization parameter $\alpha_{\rm loc}$ takes the form:

$$\alpha_{\rm loc} \simeq \frac{b}{r_0} = \frac{\sqrt{\hbar R}}{r_0(2mV_0)^{1/4}}\ , \tag{5}$$

where b is the oscillator length and $r_0 = 1.25$ fm. Using the simple liquid drop parameterization for the radius $R=r_0A^{1/3}$, one obtains [28]:

$$\alpha_{\rm loc} = \frac{\sqrt{\hbar}A^{1/6}}{(2mV_0r_0^2)^{1/4}} \simeq 0.67A^{1/6} \ . \tag{6}$$

$\alpha_{\rm loc}$ increases with $A^{1/6}$ and, therefore, one expects that cluster states are preferably formed in lighter nuclei. According to this simple expression based on a harmonic oscillator potential, the transition from coexisting cluster and mean-field states to a Fermi liquid state should occur for nuclei with $A \approx 20-30$. For heavier systems $\alpha_{\rm loc}$ is larger than 1 and, thus, heavy nuclei consist of largely delocalized nucleons characterized by a large mean-free path. The mass dependence of Eq. (6) for $\alpha_{\rm loc}$ has been verified by a fully self-consistent mean-field calculation [28] based on global nuclear energy density functionals. While a harmonic oscillator potential can be used to qualitatively analyze (de)localization of single-nucleon states, microscopic and semi-empirical energy density functionals include many-body short- and long-range correlations through their explicit dependence on nucleonic densities and, therefore, can account for the formation and stability of cluster-like substructures in nuclei [29].

Two functionals were used in the study of Ref. [28] to calculate the localization parameter for selected orbitals, as well as the values of $\alpha_{\rm loc}$ obtained by averaging the microscopic dispersions Eq. (3) for all occupied proton and neutron orbitals in the self-consistent ground-state solution. It was shown that, although both functionals reproduce empirical ground-state properties, e.g. the binding energy and charge radius, with a typical accuracy of 1%, the functional that produces a deeper self-consistent mean-field confining potential systematically predicts smaller values of $\alpha_{\rm loc}$ in lighter and medium mass nuclei and, consequently, generates equilibrium densities that are much more localized, often with pronounced cluster structures. This result is in agreement with the discussion above related to the definition of the quantality parameter $\Lambda_{\rm Mot}$ and confirms the findings of Ref. [19], where it has been shown that conditions for cluster formation can in part be traced back to the depth of the confining nuclear potential, that is, to the effective nuclear interaction. The depth of the potential determines the energy spacings between single-nucleon orbitals in deformed nuclei, the localization of the corresponding wave functions and, therefore, the degree of nucleonic density clustering.

4. Clusters in light α-conjugate nuclei

The coexistence of nuclear mean-field states and cluster structures in light nuclei is illustrated by the Ikeda diagram [16, 30, 31, 32, 4]. In a number of cases ground-state nucleonic densities display pronounced localization [29, 19], and this facilitates the formation of clusters as excited states close to the corresponding decay threshold [32, 4]. Such states cannot be isolated from the continuum of scattering states and, therefore, clusters close to the threshold belong to an open quantum system [33]. It is also well known that nuclear shape deformation plays an important role in cluster formation

because it removes the degeneracy of single-nucleon levels associated with spherical symmetry [30, 34, 35]. For instance, α clusters can be associated with isolated single-particle levels in light deformed α-conjugate systems ($N = Z$ even-even nuclei). Because of both time-invariance symmetry and isospin symmetry, two protons and two neutrons in such a level have similar wave functions, and the localization of these functions leads to an α-like structure arrangement [36, 37]. The saturation property of inter-nucleon forces, effective when both spin and isospin are coupled to zero, produces a particularly strong binding of the α cluster and a central density that is by almost a third larger than central densities in most nuclei.

The role of deformation can be exemplified by performing self-consistent mean-field calculations based on nuclear energy density functionals (EDFs), with constraints on the mass multipole moments of a nucleus. The corresponding single-nucleon Kohn-Sham equations (Schrödinger for non-relativistic functionals, or Dirac for relativistic EDFs, with the Hamiltonian defined as the functional derivative of the corresponding EDF with respect to density) are solved in the intrinsic frame of reference attached to the nucleus, in which the shape of the nucleus can be arbitrarily deformed. The result are static symmetry-breaking product many-body states, and in the examples below we consider configurations that are obtained by breaking both the axial and reflection symmetries. Even though the many-body system is determined by a very large number of microscopic states, these can be organised in a collection of basins on the deformation energy surface, that are robust to small external perturbations [38]. In the present illustrative calculation nuclear shapes are characterized by mass quadrupole and octupole moments that can be related to the polar quadrupole deformation parameters (β_2, γ), and the axial and triaxial octupole parameters (β_{30}, β_{32}), respectively. In the examples considered in this section different shapes correspond to global or local minima on the $(\beta_2, \gamma, \beta_{30}, \beta_{32})$ energy hypersurface.

Figure 1 displays the self-consistent intrinsic densities of ^{20}Ne, calculated using the relativistic Hartree-Bogoliubov model (RHB) [40] based on the energy density functional DD-ME2 [39]. For the examples considered in the present work, pairing correlations have been taken into account by employing an interaction that is separable in momentum space, and is completely determined by two parameters adjusted to reproduce the empirical bell-shaped pairing gap in symmetric nuclear matter [41]. The reflection-asymmetric axial density shown in the upper panel is obtained by imposing constraints on both the axial quadrupole and octupole deformation parameters β_2 and β_{30}, respectively. $\beta_2 = 0.55$ corresponds to the equilibrium quadrupole deformation, and $\beta_{30} = 0.50$. The intrinsic density exhibits the structure of an ^{16}O core plus the α-cluster. In the lower panel we plot the corresponding axially and reflection symmetric equilibrium nucleon density distribution of ^{20}Ne. This quadrupole deformed shape is characterized by two regions of pronounced localization at the outer ends of the symmetry axis and an oblate deformed core, that is, a quasimolecular α-^{12}C-α structure.

The identification of cluster structures from nucleonic density distributions, as shown in Ref. [29], often misses important aspects of many-body dynamics, such as

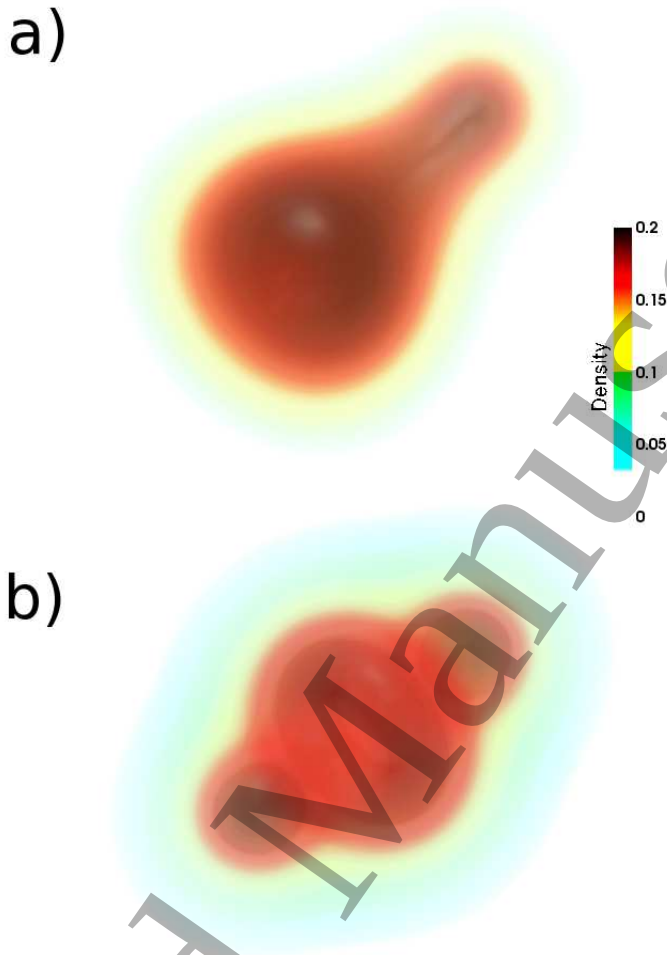

Figure 1. Self-consistent deformation-constrained axially symmetric intrinsic densities of ^{20}Ne. The octupole deformed density in the upper panel is reflection asymmetric. Adapted from references [28] and [34].

the kinetic energy density or density gradients. Therefore, an alternative localization measure, originally developed for the analysis of bonding structures in molecules [42], has been applied in Refs. [29, 43] to α-clustering in light nuclei. The nucleon localization function can be derived by considering the conditional probability of finding a nucleon within a distance δ from a given nucleon at point $\vec{r}$ with the same spin σ (=↑ or ↓) and isospin q (= n or p) quantum numbers [29]:

$$R_{q\sigma}(\vec{r},\delta) \approx \frac{1}{3}\left(\tau_{q\sigma} - \frac{1}{4}\frac{|\vec{\nabla}\rho_{q\sigma}|^2}{\rho_{q\sigma}} - \frac{\vec{j}_{q\sigma}^{\,2}}{\rho_{q\sigma}}\right)\delta^2 + \mathcal{O}(\delta^\ni), \tag{7}$$

where $\rho_{q\sigma}$, $\tau_{q\sigma}$, $\vec{j}_{q\sigma}$, and $\vec{\nabla}\rho_{q\sigma}$ denote the particle density, kinetic energy density, current density, and density gradient, respectively, that are completely determined by the self-consistent mean-field single-particle states. A small conditional probability indicates a high degree of localization of the reference nucleon. The corresponding dimensionless

and normalized expression for the localization measure can be expressed by the following relation:

$$C_{q\sigma}(\vec{r}) = \left[1 + \left(\frac{\tau_{q\sigma}\rho_{q\sigma} - \frac{1}{4}|\vec{\nabla}\rho_{q\sigma}|^2 - \vec{j}^2_{q\sigma}}{\rho_{q\sigma}\tau^{\rm TF}_{q\sigma}}\right)^2\right]^{-1}, \tag{8}$$

With the Thomas-Fermi kinetic energy density $\tau^{\rm TF}_{q\sigma} = \frac{3}{5}(6\pi^2)^{2/3}\rho^{5/3}_{q\sigma}$ in the denominator, the function $C_{q\sigma}(\vec{r})$ is normalized and provides a dimensionless measure of nucleon localization. For homogeneous nuclear matter $\tau = \tau^{\rm TF}_{q\sigma}$, the second and third term in the numerator vanish, and $C_{q\sigma} = 1/2$. In the other limit $C_{q\sigma}(\vec{r}) \approx 1$ indicates that the probability of finding two nucleons with the same spin and isospin at the same point $\vec{r}$ is very small. This is precisely the case for the α-cluster of four particles: $p\uparrow$, $p\downarrow$, $n\uparrow$, and $n\downarrow$, for which all four nucleon localization functions $C_{q\sigma} \approx 1$.

In Fig. 2 we plot the proton localization function $C_{p\uparrow}$ (left panel) and total intrinsic nucleon density (right panel) in the $x-z$ plane for ^{20}Ne, calculated with the relativistic energy density functional DD-ME2. For this case time-reversal states are equally occupied and the current density $\vec{j}_{q\sigma}$ in Eq. (8) vanishes. The localization functions are identical for spin-up and spin-down nucleons and, since the Coulomb contribution is small, the neutron and proton localization functions are also very similar. One notices that even though the single-nucleon density already indicates the formation of α clusters in the axially symmetric configurations, it is the localization function that clearly identifies the regions with $C_{p\uparrow}(\vec{r}) \approx 1$ on the elongation axis: the α-^{16}O structure in the upper panel, and a ring at the center for the α-^{12}C-α structure in the lower panel. This result is similar to the one obtained in Ref. [29] using a Skyrme energy density functional, and where it was also emphasized that $C_{q\sigma}(\vec{r})$ provides an excellent measure of correlation and localization because it includes the dependence on the kinetic energy of the relative motion of spin-parallel nucleons at a particular point in space.

The pronounced density peaks enhance the probability of formation of α-clusters in excited states close to the energy threshold for α-particle emission [16, 30, 33, 35]. This is illustrated in Fig. 3 where we display various cluster shapes in α-conjugate nuclei, obtained in triaxial and reflection-asymmetric self-consistent calculations based on the functional DD-ME2. Densities that correspond to positive-parity projected intrinsic states are arranged in order of increasing energy. The lowest configurations correspond to equilibrium density distributions [35]. In analogy to the original Ikeda diagram [16], these microscopic self-consistent density distributions emphasize the coexistence of the nuclear mean-field and cluster structures that appear near or above the α dissociation threshold energy.

Exotic structures of α clusters (chains and rings) can be stabilized in a rotating nucleus by a competition between the nuclear attractive and centrifugal forces [44]. A microscopic study of this phenomenon can be performed, for instance, by using cranked self-consistent mean-field methods. The cranked self-consistent equation in the rotating intrinsic frame is obtained variationally: $\delta < H - \boldsymbol{\omega}\cdot\boldsymbol{J} >= 0$, where H is the total Hamiltonian in the laboratory frame, $\boldsymbol{\omega}$ is the rotational frequency, and $\boldsymbol{J}$ the angular

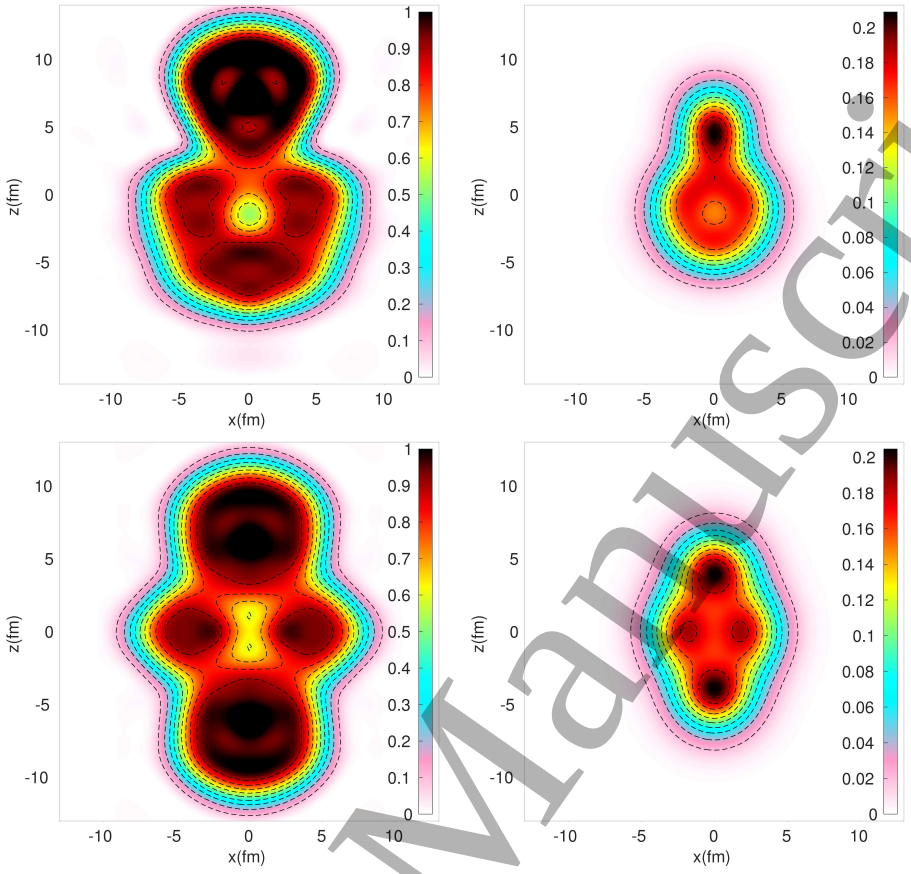

Figure 2. Proton localization function (left) and total density (in nucleon/fm^3, right) in the $x-z$ plane for ^{20}Ne. The top and bottom panels correspond to the reflection asymmetric (octupole) and reflection symmetric (quadrupole) shapes, respectively, shown in Fig. 1.

momentum. Within this general framework a variety of models based on energy density functionals or effective nuclear interactions have been used to analyze the stability of chain and ring configurations in relation to angular momentum. Among a number of interesting recent studies, it has been shown that in a region of angular momentum ($13\hbar - 18\hbar$) the chain of four α clusters is stabilized in ^{16}O [45, 46]; the stability of rod-shaped structures has been analyzed for ^{24}Mg [47] and carbon isotopes [48]; and a systematic investigation of extremely deformed structures in $N \approx Z$ nuclei of the $A \approx 40$ mass region has been performed [49].

Figs. 1 – 3 exhibit localized, crystal-like cluster structures, characteristic for the self-consistent mean-field method used to calculate nuclear deformation energy hypersurfaces. The corresponding self-consistent solutions contain the energy of spurious center-of-mass motion of each cluster that needs to be subtracted from the total energy. By restoring symmetries broken by the mean-field (translational, rotational, and parity in the case of octupole deformations), and allowing for configuration mixing, solutions that correspond to non-localized clusters are obtained. Non-localized clustering has

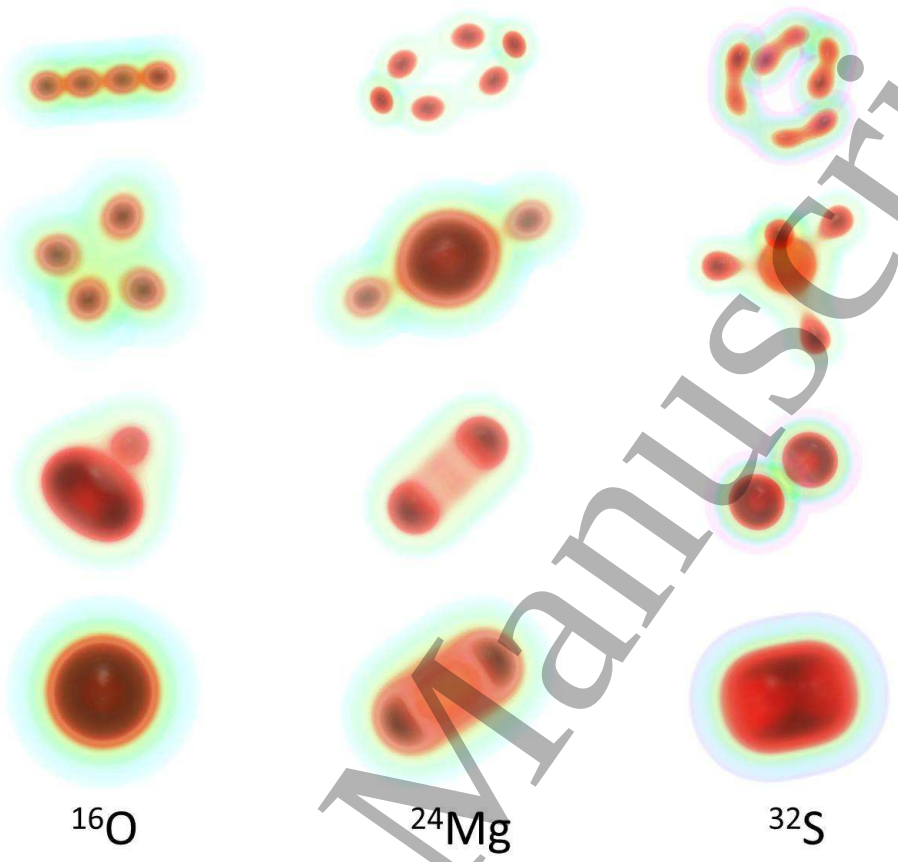

Figure 3. Intrinsic densities of deformation-constrained configurations in $N = Z$ nuclei. For each nucleus the density in the bottom row corresponds to the equilibrium configuration, and excited configurations are displayed in order of increasing energy. Adapted from reference [35].

extensively been investigated using an angular-momentum-projected version of the Tohsaki-Horiuchi-Schuck-Röpke (THSR) wave function [50, 51, 52, 6]. In light nuclei at low densities α-like clusters display a strong tendency to condense in the same orbital with respect to their center-of-mass motion. The best known example is the second 0^+ state in ^{12}C at 7.65 MeV [53] – the Hoyle state that plays a key role in stellar nucleosynthesis – and can be considered as a weakly interacting gas of 3 α particles. It is located at an excitation energy that is ≈ 300 keV above the threshold at which ^{12}C dissociates into 3 α particles, and it is quasi-bound by the Coulomb barrier. In fact, the wave function of this state can be described with 70% probability as a product state of α particles, all in the lowest $0S$ state [54, 55, 6]. One could consider this state as an α-boson condensate [56] taking into account, of course, that it belongs to a finite system with a small number of particles. In fact, microscopic calculations indicate that the relative positions of the clusters are correlated and, therefore, the Hoyle state can only qualitatively be interpreted as a boson condensate [57].

The formation of an α-condensate can occur at an excitation energy that corresponds to the threshold at which all α particles become unbound. Cluster gas states near the $n\alpha$ dissociation threshold energy and α particle condensation in heavier α-conjugate nuclei is a topic of great current interest, both theoretical and experimental [58, 4, 59, 23, 60, 51]. An interesting question is how many α particles can be bound in a dilute finite nuclear system, that is, what is the critical number of α bosons in condensed states beyond which the system becomes unbound [61]? Starting from ^{12}C, for instance, and adding more α clusters, the total energy of the $N\alpha$ gas state increases because of the competition between the short-range attractive $\alpha-\alpha$ nuclear potential and the long-range repulsive Coulomb potential. With increasing the number of charged α bosons the repulsive potential becomes dominant, the system expands and the average distance between α particles increases. The Coulomb potential barrier confining the α clusters gradually decreases and, at some critical value N_c, the self-trapped system becomes unbound. In the phenomenological study of Ref. [61] it has been shown that $N\alpha$ states with $J = 0^+$ in α-conjugate nuclei from ^{12}C to ^{40}Ca occur at excitation energies below 20 MeV, and the critical number of α bosons is $N_c \approx 10$.

More generally, we emphasize the role of the saturation property of inter-nucleon interactions in the mechanism of cluster formation in finite nuclei and in dilute nuclear matter. In excited configurations of light deformed nuclei the nucleon density is reduced along the deformation axis with respect to the equilibrium. This favors the formation of clusters because it locally enhances the nucleonic density toward its saturation value, therefore increasing the binding of the system. For a relatively light nucleus, and especially for α-conjugate systems, the most effective way to increase the density locally is the clustering of nucleons into α particles. Because of saturation the interaction between α-clusters is weak and excited states near the $n\alpha$ threshold energy can be described as a gas of α-clusters. In fact, when the density of nucleonic matter is reduced below its equilibrium values, saturation causes a Mott-like transition to a hybrid phase composed of clusters of α-particles. This effect has been investigated in self-consistent mean-field calculations of even-even $N = Z$ nuclei, with a restriction to spherically symmetric configurations[62, 35]. It has been shown that by expanding an $n-\alpha$ nucleus the corresponding total energy as a function of the nuclear radius goes over a maximum before reaching the asymptotic low density limit of a gas of α-particles.

This transition is illustrated in Fig. 4, where we display the result of a constrained self-consistent mean-field calculation of ^{16}O, using the relativistic functional DD-ME2. The equilibrium mean-field solution reproduces the empirical binding energy and charge radius of ^{16}O. A constraint on the nuclear radius is used to gradually reduce the nucleon density by inflating the spherical nucleus. As the size of the nucleus becomes larger the total energy of the system increases with respect to the equilibrium configuration. When the density is reduced to $\rho/\rho_{\rm eq} \approx 1/3$, the system undergoes a Mott-like phase transition [25, 62, 35] to a configuration of 4 α-particles. As shown in Fig. 4, this transition occurs at a radius of $r_c = 3.33$ fm, with the corresponding ratio of the critical radius to the ground-state radius $r_c/r_{g.s.} \approx 1.3$. Experimental evidence for α-particle

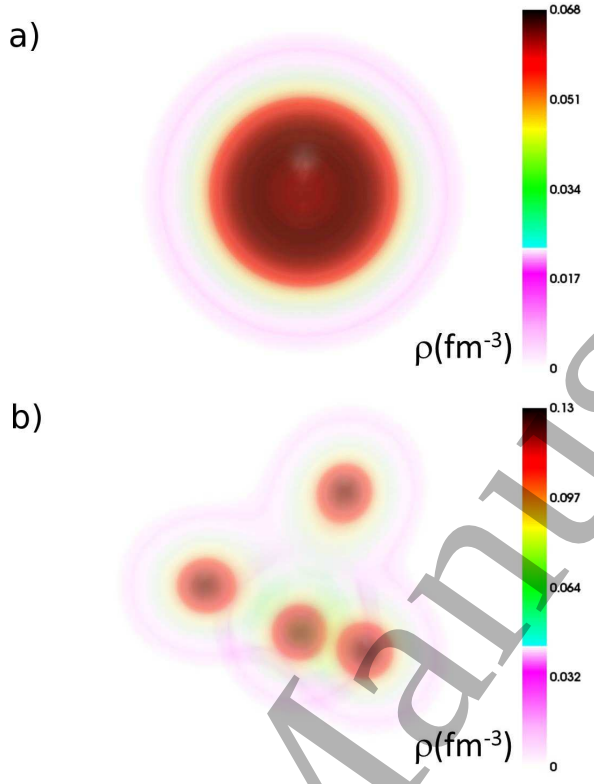

Figure 4. Self-consistent intrinsic nucleon density of ^{16}O for a radius constrained to 3.32 fm (a) and 3.34 fm (b). Reprinted from reference [34].

clustering (simultaneous emission) in excited expanding $N\alpha$ source nuclei ^{16}O, ^{20}Ne and ^{24}Mg, was recently reported in a study of fragmentation of quasi-projectiles from the nuclear reaction ^{40}Ca on ^{12}C [63].

5. Clustering in neutron-rich nuclei

In addition to $N = Z$ systems, a particularly interesting topic is the formation of clusters in unstable neutron-rich nuclei. In a number of light $N > Z$ nuclei low-energy cluster structures can be described by molecular bonding of α-particles by the excess neutrons [30, 31, 4, 5, 64]. The conditions for the formation of molecular states include the presence of strongly bound α-cores, a weakly attractive $\alpha - \alpha$ potential which becomes repulsive at small distances, and additional weakly-bound single-particle orbitals occupied by valence neutrons [65]. Decomposing the total nucleon density into the α clusters and the density of additional valence neutrons, one obtains a picture of nuclear molecular states. For covalent bonding, a negative-parity neutron orbital perpendicular to the $\alpha - \alpha$ axis is called a π-orbital, whereas a σ-orbital denotes a positive-parity orbital parallel to the $\alpha - \alpha$ direction [65, 5, 66]. While "molecular orbits" of valence neutrons characterize cluster structures at threshold energies (covalent bonding), at higher excitation energies excess neutrons tend to form atomic orbits

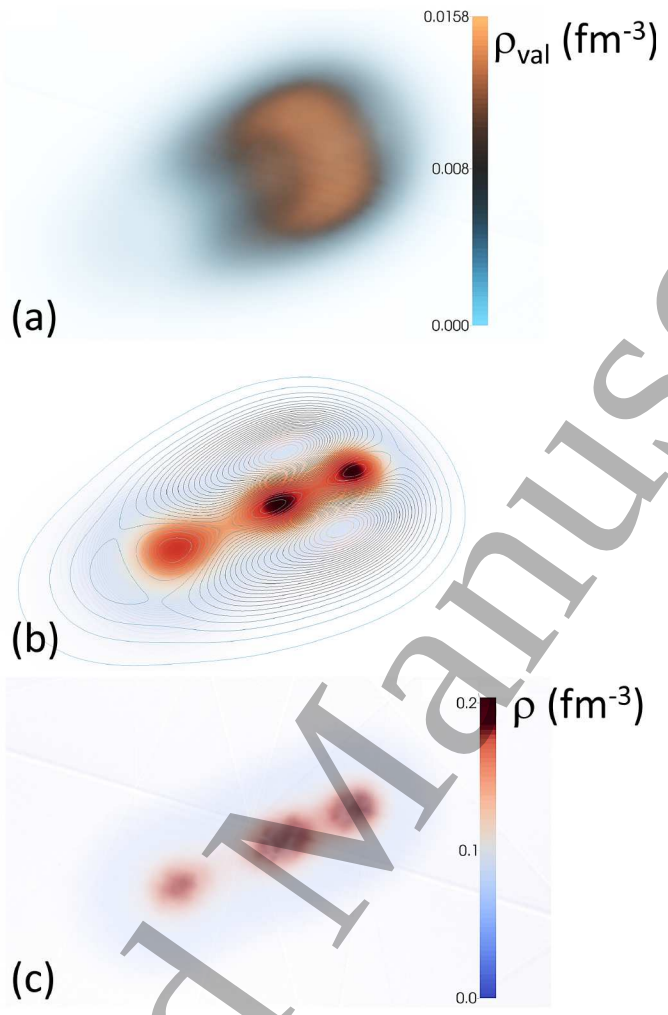

Figure 5. Nucleonic densities for an excited configuration of ^{14}C: (a) 3D density of the valence neutrons; (b) contour plots of the density of the valence neutrons and the $\alpha+\alpha+\alpha$ core density in the (Oxz) plane; (c) 3D density of the $\alpha+\alpha+\alpha$ core.

around individual clusters (ionic bonding) [4, 5].

Even though detailed spectroscopic properties of molecule-like structures in neutron-rich nuclei can only be described using structure models that take into account correlations related to the restoration of symmetries broken by the nuclear mean field, such as the antisymmetrized molecular dynamics (AMD) approach [4, 5], basic concepts can already be illustrated in a simple self-consistent mean-field calculation based on global functionals. As an example we consider cluster structures in excited states of neutron-rich carbon isotopes [35]. A study based on the microscopic molecular-orbit (MO) $\alpha+\alpha+\alpha+n+n+\ldots$ model [67] has shown that valence neutrons in the π-orbit increase the binding energy and stabilize the linear chain of 3 α against the breathing-like breakup. In Figs. 5 and 6 we show the excess-neutron molecular orbits in excited configurations of ^{14}C and ^{16}C, calculated using the self-consistent microscopic approach based on the relativistic energy density functional DD-ME2. The plot of the density of

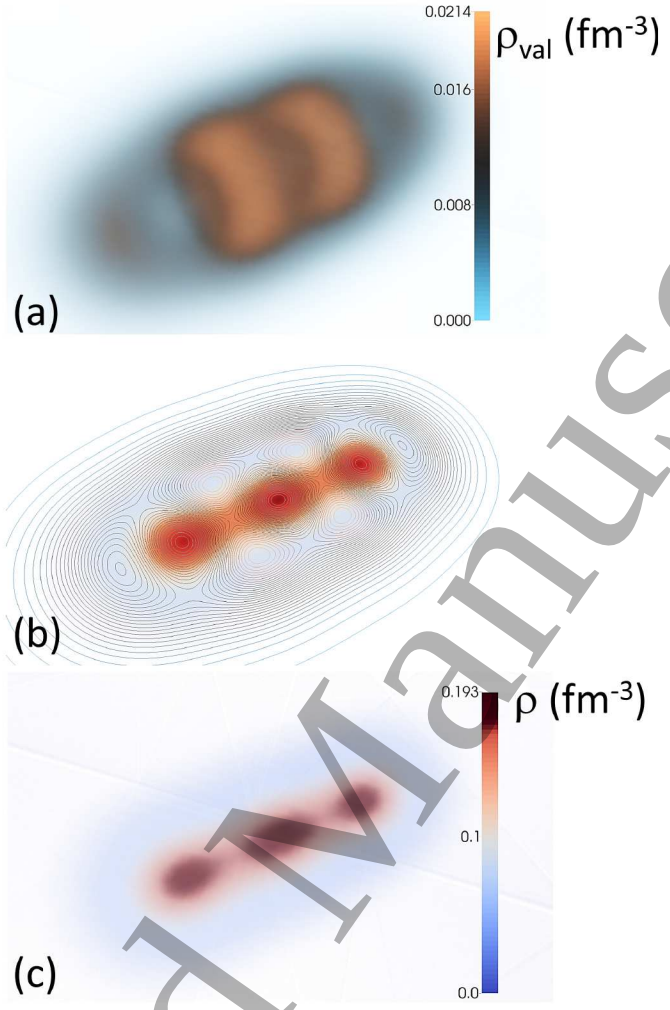

Figure 6. Same as in the caption to Fig. 5 but for an excited configuration of ^{16}C.

an excited configuration of ^{14}C in terms of the 3 α clusters and the two valence neutrons is shown in Fig 5. In this case correlations between the valence neutrons tend to favor a reflection asymmetric chain configuration: $\alpha-2n-\alpha-\alpha$, with the two valence neutrons forming a π-bond between two α clusters. This configuration is predicted at somewhat lower excitation energy than the reflection symmetric chain $\alpha-n-\alpha-n-\alpha$. A reflection-symmetric configuration with four valence neutrons: $\alpha-2n-\alpha-2n-\alpha$ is favored in ^{16}C, as shown Fig 6. Similar results have also been obtained with the antisymmetrized molecular dynamics (AMD) model in Ref. [68], and we note that strong evidence for linear-chain cluster states in ^{14}C has very recently been observed in a ^{16}Be+α resonant scattering experiment reported in [69].

6. Spin-orbit coupling in bound fermion systems

The localization of nucleons in finite nuclear systems and, therefore, the conditions for the formation and coexistence of cluster structures and the nuclear mean-field can

be related to the depth of the confining single-nucleon potential [19]. This potential determines the energy spacings of the corresponding single-nucleon spectra and, in particular, the energy gaps between major shells. In the following a connection is established with another important effect that characterizes spectroscopic properties of bound quantum systems such as atoms, nuclei, hypernuclei, quarkonia, etc., and which arises from the spin-orbit coupling. Depending on the specific system under consideration, the spin-orbit interaction is large in nuclei, small in quarkonia, perturbative in atoms. In nuclei the strong coupling between the orbital angular momentum and spin of a nucleon accounts for the empirical magic numbers, and the energy spacings between spin-orbit partner states can be as large as the gaps between major shells.

Nucleons are Dirac particles and, in the relativistic mean-field approximation [70, 71], the single-nucleon dynamics is governed by the Dirac equation:

$$\left[\vec{\alpha}\cdot\vec{p}+V+\beta(m+S)\right]\psi_i = E_i\psi_i \tag{9}$$

where ψ denotes the single-nucleon Dirac spinor:

$$\begin{pmatrix}\phi\\ \chi\end{pmatrix} \tag{10}$$

and m is the nucleon mass . Here we only consider spherical nuclei and assume time-reversal symmetry (pairwise occupied states with Kramers degeneracy), which ensures that the only non-vanishing components of the vector fields are the time-like ones and thus there is no net contribution from nucleon currents. The local self-consistent vector V and scalar S potentials are uniquely determined by the actual nucleon density and scalar density of a given nucleus, respectively. In the standard non-relativistic reduction of the single-particle Dirac equation, the single-particle mean-field equation takes a Schrödinger-like form which, in addition to the confining potential, exhibits the spin-orbit potential explicitly:

$$\left[\vec{p}\frac{1}{2\mathcal{M}(r)}\vec{p}+U(r)+V^{LS}(r)\right]\phi = \varepsilon\phi\ , \tag{11}$$

where $\mathcal{M}(r)\equiv m+\left(S(r)-V(r)\right)/2$ is the nucleon effective mass, $U(r)\equiv V(r)+S(r)$, and the spin-orbit potential:

$$V^{LS}\equiv\frac{1}{2\mathcal{M}^2(r)}\frac{1}{r}\frac{d}{dr}\left(V(r)-S(r)\right)\vec{l}\cdot\vec{s}\,. \tag{12}$$

The effective nuclear spin-orbit potential, therefore, originates from the difference between the vector potential V (short-range repulsion) with typical strength of ≈ 350 MeV, and the scalar potential S (medium-range attraction), typically of the order of -400 MeV in nucleonic matter and finite nuclei. The sum of these two fields $V+S\approx -50$ MeV provides the confining single-nucleon potential and, therefore, determines the energy spacings between major shells. The large difference $V-S\approx 750$ MeV, on the other hand, governs the splitting between spin-orbit partner states in finite nuclei, which are also of the order of MeV. In fact, when considering the ratio between the

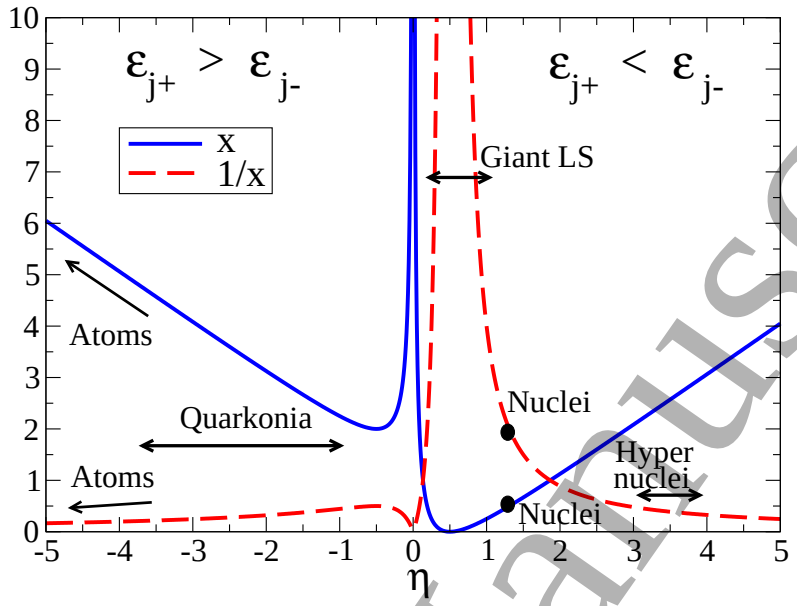

Figure 7. The ratio between the principal energy spacings and the spin-orbit splittings (fine structure) as a function of the ratio η between the mass of the particle and the effective potential that determines the spin-orbit force in a given quantum system. Adapted from reference [72].

energy spacings $\hbar\omega_0$ characterized by principal single-particle quantum numbers and the energy splitting of spin-orbit partners, it can be shown that [72]:

$$x \equiv \frac{\hbar\omega_0}{|\Delta < V^{LS} > |} = K\left|\eta - 1 + \frac{1}{4\eta}\right| , \tag{13}$$

where $K = \sqrt{-2mU_0}R_0/l\hbar$, $U_0 \equiv U(r=0) = V(0) + S(0)$ is the depth of the potential, $R_0 = r_0 A^{1/3}$ ($r_0 \approx 1.2$ fm) is the nuclear radius, l denotes the orbital angular momentum, and

$$\eta \equiv \frac{m}{V - S} . \tag{14}$$

Since for the nucleon mass $m \approx 940$ MeV and $V - S \approx 750$ MeV: $\eta = 1.25$, and it follows from Eq. (13) that the ratio x is of the order $1 - 5$, that is, in nuclei the energy splitting between spin-orbit partner states is comparable in magnitude to the spacings between major oscillator shells.

In Fig. 7 we plot the ratio between the principal energy spacings and the spin-orbit splittings for different systems of bound fermions, as a function of the parameter η:

$$x \simeq \left|\eta - 1 + \frac{1}{4\eta}\right| . \tag{15}$$

In general, η is the ratio between the mass of the particle and the effective potential whose gradient determines the spin-orbit force in a given quantum system. In nuclei the

near equality of the mass of the nucleon and the difference between the large repulsive vector and attractive scalar potentials explains the fact that the spin-orbit splittings are comparable to the energy spacing between major oscillator shells. The same universal functional form also applies to other bound quantum systems, regardless of whether the spin-orbit potential originates from the strong or electromagnetic interaction, and for which the ratio between the principal energy spacings and the spin-orbit splittings is orders of magnitude larger than in the nuclear case [72].

A special case arises when the mass of the particle is close to $(V - S)/2$. This implies $\eta \simeq 1/2$ and, thus, $x = 0$. The energy spacings between bound states are then characterized by very large spin-orbit coupling (giant LS). Such states could be generated in particular situations when the strength of the effective potential whose gradient determines the spin-orbit force can be treated as an external parameter.

The spin-orbit parameter η can be related to the quantality $\Lambda_{\rm Mot}$ Eq. (1) by defining an effective coupling strength:

$$\alpha_{eff} \hat{=} \frac{U_0 r_0}{\hbar c} \tag{16}$$

where U_0 is the depth of the confining potential and r_0 its effective range. It can then be easily shown that the following relation holds to a good approximation:

$$\eta \Lambda_{\rm Mot} \alpha_{eff}^2 \approx 1 \, . \tag{17}$$

By increasing the depth of the potential, the quantality parameter decreases reflecting an enhanced localization. In this case the spin-orbit parameter η is also reduced because of the increase of the gradient of the effective potential, and this leads to an enhancement of the energy spacings between spin-orbit partner states.

7. Summary and outlook

Nucleon localization, conditions for formation of cluster structures in the nuclear medium, their composition, stability and decay properties present a recurrent theme in nuclear physics, and nucleon clustering plays a key role in understanding the process of stellar nucleosynthesis. In this article we discussed some recent issues in a microscopic theoretical description of the generic phenomenon of cluster formation in finite nuclei based on the concept of nucleon localization.

Extended nucleonic matter at equilibrium behaves like a Fermi liquid, whereas in the low-density limit, in chemical equilibrium and at low temperatures, four-nucleon correlations lead to a condensation of α-particles. Finite nuclei, as self-bound and open quantum systems, exhibit both quantum liquid-drop and cluster features. As a measure of nucleon localization and cluster-liquid transition, we have analyzed a dimensionless ratio between the spatial dispersion of the single-nucleon wave function and the average inter-nucleon distance. It has been shown that conditions for nucleon localization and formation of clusters can be related to the depth of the effective confining potential, that is, to the effective nuclear interaction. In addition to nucleon

densities, an alternative localization function has been explored that explicitly includes a dependence on the kinetic energy density and density gradients. We have particularly emphasized the role of the saturation property of the inter-nucleon interaction in the mechanism of cluster formation in finite nuclei, and the effect of deformation in the formation of clusters as excited states has been illustrated by performing fully self-consistent mean-field calculations, with constraints on the multipole moments of the nucleon density distribution. An interesting topic that we have briefly illustrated is the formation of molecular bonds of α-clusters by excess neutrons in neutron-rich light nuclei. The localization of nucleons is particularly reflected in the energy spacings of the corresponding single-nucleon spectra, and a relation has been established between the localization (quantality) parameter and a quantity that characterizes the large energy spacings between spin-orbit partner states in nuclei.

Even though in recent years important advances have been made in understanding localization and clustering phenomena, many open issues remain to be explored, both theoretically and experimentally. These include, in particular, spectroscopy above the α-decay threshold in light nuclei, the occurrence of cluster structures in neutron-rich nuclei far from the valley of β-stability, exotic cluster structures stabilized by the rotation of the deformed nuclear system, cluster gas states and α-cluster condensation, formation of nucleon clusters in heavy nuclei, clustering in nuclear reactions including those important for astrophysical applications, and the development of *ab initio* theoretical methods that can describe both the formation of the nuclear mean-field and clustering characteristics of many-nucleon dynamics in finite nuclei.

Acknowledgments

This work has been supported in part by the Croatian Science Foundation – project "Structure and Dynamics of Exotic Femtosystems" (IP-2014-09-9159) and by the QuantiXLie Centre of Excellence.

[1] C. Beck, Clusters in Nuclei, Vol. 1, Lecture Notes in Physics **818** (Springer, 2010).
[2] C. Beck, Clusters in Nuclei, Vol. 2, Lecture Notes in Physics **848** (Springer, 2012).
[3] C. Beck, Clusters in Nuclei, Vol. 3, Lecture Notes in Physics **875** (Springer, 2014).
[4] H. Horiuchi, K. Ikeda, and K. Kato, Prog. Theor. Phys. Supplement **192**, 1 (2012).
[5] M. Kimura, T. Suhara, and Y. Kanada-En'yo, Eur. Phys. J. A **52**, 43 (2016).
[6] A. Tohsaki, H. Horiuchi, P. Schuck, and G. Röpke, Rev. Mod. Phys. **89**, 011002 (2017).
[7] M. Freer, H. Horiuchi, Y. Kanada-En'yo, D. Lee, and U.-G. Meissner, arXiv:1705.06192.
[8] D. G. Ravenhall, C. J. Pethick, and J. R. Wilson, Phys. Rev. Lett. **50**, 2066 (1983).
[9] M. Hashimoto, H. Seki, and M. Yamada, Prog. Theor. Phys. **71**, 320 (1984).
[10] C. P. Lorenz, D. G. Ravenhall, and C. J. Pethick, Phys. Rev. Lett. **70**, 379 (1993).
[11] J. A. Wheeler, Phys. Rev. **52**, 1107 (1937).
[12] C. F. V. Weizsäcker, Naturwissenschaften **26**, 209 (1938).
[13] L. R. Hafstad, and E. Teller, Phys. Rev. **54**, 681 (1938).
[14] D. M. Dennison Phys. Rev. **57**, 454 (1940).
[15] H. Morinaga, Phys. Rev. **101**, 254 (1956).
[16] K. Ikeda, N. Takigawa, and H. Horiuchi, Prog. Theor. Phys. Supplement **E68**, 464 (1968).

[17] T. Neff, and H. Feldmeier, Eur. Phys. J. Special Topics **156**, 69 (2008).
[18] S. Elhatisari et al., Phys. Rev. Lett. **117**, 132501 (2016).
[19] J.-P. Ebran, E. Khan, T. Nikšić, and D. Vretenar, Nature **487**, 341 (2012).
[20] B. R. Mottelson, in: Nuclear Structure, Les Houches, Session LXVI, 25 (1996).
[21] J. de Boer, Physica **14**, 139 (1948).
[22] B. R. Mottelson, Nuc. Phys. A **649**, 45c (1999).
[23] N. T. Zinner and A. S. Jensen, J. Phys. G: Nucl. Part. Phys. **40**, 053101 (2013).
[24] G. Röpke, A. Schnell, P. Schuck, and P. Noziéres, Phys. Rev. Lett. **80**, 3177 (1998).
[25] S. Typel, G. Röpke, T. Klähn, D. Blaschke, and H. H. Wolter, Phys. Rev. C **81**, 015803 (2010).
[26] H. Pais, and S. Typel, arXiv:1612.07022
[27] D. Pines and P. Noziéres, The theory of quantum liquids, (Benjamin Inc., 1966).
[28] J.-P. Ebran, E. Khan, T. Nikšić, and D. Vretenar, Phys. Rev. C **87**, 044307 (2013).
[29] P.-G. Reinhard, J. A. Maruhn, A. S. Umar, and V. E. Oberacker, Phys. Rev. C **83**, 034312 (2011).
[30] W. von Oertzen, M. Freer, and Y. Kanada-En'yo, Phys. Rep. **432**, 43 (2006).
[31] M. Freer, Rep. Prog. Phys. **70**, 2149 (2007).
[32] H. Horiuchi, in: Clusters in Nuclei, Vol. 1, edited by C. Beck, Lecture Notes in Physics **818**, 57 (Springer, 2010).
[33] J. Okolowicz, M. Ploszajczak, and W. Nazarewicz, Prog. Theor. Phys. Supplement **196**, 230 (2012).
[34] J.-P. Ebran, E. Khan, T. Nikšić, and D. Vretenar, Phys. Rev. C **89**, 031303(R) (2014).
[35] J.-P. Ebran, E. Khan, T. Nikšić, and D. Vretenar, Phys. Rev. C **90**, 054329 (2014).
[36] S. Åberg and L.-O. Jönsson, Z. Phys. A **349**, 205 (1994).
[37] M. Freer, R. R. Betts, and A. H. Wuosmaa, Nucl. Phys. A **587**, 36 (1995).
[38] R. B. Laughlin, D. Pines, J. Schmalian, B. P. Stojković, and P. Wolynes, Proc. Natl. Acad. Sci. **97**, 32 (2000).
[39] G. A. Lalazissis, T. Nikšić, D. Vretenar, and P. Ring, Phys. Rev. C **71**, 024312 (2005).
[40] D. Vretenar, A. V. Afanasjev, G. A. Lalazissis, and P. Ring, Phys. Rep. **409**, 101 (2005).
[41] T. Nikšić, P. Ring, D. Vretenar, Y. Tian, and Z. Y. Ma, Phys. Rev. C **81**, 054318 (2010).
[42] A. D. Becke, and K. E. Edgecombe, J. Chem. Phys. **92**, 5397 (1990).
[43] C. L. Zhang, B. Schuetrumpf, and W. Nazarewicz, Phys. Rev. C **94**, 064323 (2016).
[44] D. H. Wilkinson, Nucl. Phys. A **452**, 296 (1986).
[45] T. Ichikawa, J. A. Maruhn, N. Itagaki, and S. Ohkubo, Phys. Rev. Lett. **107**, 112501 (2011).
[46] J. M. Yao, N. Itagaki, and J. Meng, Phys. Rev. C **90**, 054307 (2014).
[47] Y. Iwata, T. Ichikawa, N. Itagaki, J. A. Maruhn, and T. Otsuka, Phys. Rev. C **92**, 011303(R) (2015).
[48] P. W. Zhao, N. Itagaki, and J. Meng, Phys. Rev. Lett. **115**, 022501 (2015).
[49] D. Ray and A. V. Afanasjev, Phys. Rev. C **94**, 014310 (2016).
[50] A. Tohsaki, H. Horiuchi, P. Schuck, and G. Röpke, Phys. Rev. Lett. **87**, 192501 (2001).
[51] B. Zhou, Y. Funaki, H. Horiuchi, Z. Ren, G. Röpke, P. Schuck, A. Tohsaki, C. Xu, and T. Yamada, Phys. Rev. Lett. **110**, 262501 (2013), and Phys. Rev. C **89**, 034319 (2014).
[52] M. Lyu, Z. Ren, B. Zhou, Y. Funaki, H. Horiuchi, G. Röpke, P. Schuck, A. Tohsaki, C. Xu, and T. Yamada, Phys. Rev. C **93**, 054308 (2016).
[53] M. Freer, and H. O. U. Fynbo, Prog. Part. Nucl. Phys **78**, 1 (2014).
[54] H. Matsumara and Y. Suzuki, Nucl. Phys. A **739**, 238 (2004).
[55] T. Yamada and P. Schuck, Eur. Phys. J. A **26**, 185 (2005).
[56] T. Yamada, Y. Funaki, H. Horiuchi, G. Röpke, P. Schuck, and A. Tohsaki, in: Clusters in Nuclei, Vol. 2, edited by C. Beck, Lecture Notes in Physics **848**, 165 (Springer, 2012).
[57] M. Chernykh, H. Feldmeier, T. Neff, P. von Neumann-Cosel, A. Richter, Phys. Rev. Lett. **98**, 032501 (2007).
[58] Y. Funaki, M. Girod, H. Horiuchi, G. Röpke, P. Schuck, A. Tohsaki, and T. Yamada, J. Phys. G: Nucl. Part. Phys. **37**, 064012 (2010).
[59] N. T. Zinner and A. S. Jensen, Phys. Rev. C **78**, 041306(R) (2008).

[60] W. von Oertzen, in: Clusters in Nuclei, Vol. 1, edited by C. Beck, Lecture Notes in Physics **818**, 109 (Springer, 2010).
[61] T. Yamada and P. Schuck, Phys. Rev. C **69**, 024309 (2004).
[62] M. Girod and P. Schuck, Phys. Rev. Lett. **111**, 132503 (2013).
[63] B. Borderie et al., Phys. Lett. B **755**, 475 (2016).
[64] W. von Oertzen and M. Milin, in: Clusters in Nuclei, Vol. 3, edited by C. Beck, Lecture Notes in Physics **875**, 147 (Springer, 2014).
[65] W. von Oertzen, Eur. Phys. J. A **11**, 403 (2001).
[66] Y. Kanada-En'yo, Phys. Rev. C **85**, 044320 (2012).
[67] N. Itagaki, S. Okabe, K. Ikeda, and I. Tanihata, Phys. Rev. C **64**, 014301 (2001).
[68] Y. Kanada-En'yo and H. Horiuchi, Prog. Theor. Phys. Supplement **142**, 205 (2001).
[69] H. Yamaguchi et al., Phys. Lett. B **766**, 11 (2017).
[70] B. D. Serot and J. D. Walecka, Adv. Nucl. Phys. **16**, 1 (1986), Int. J. Mod. Phys. E **6**, 515 (1997).
[71] D. Vretenar, A. V. Afanasjev, G. A. Lalazissis, and P. Ring, Phys. Rep. **409**, 101 (2005).
[72] J.-P. Ebran, E. Khan, A. Mutschler, and D. Vretenar, J. Phys. G: Nucl. Part. Phys. **43**, 085101 (2016).